Journal of Hydrology 564 (2018) 1048–1057

Contents lists available at ScienceDirect

Journal of Hydrology

journal homepage: www.elsevier.com/locate/jhydrol

Research papers

# District-level assessment of the ecohydrological resilience to hydroclimatic disturbances and its controlling factors in India

Ashutosh Sharma[a], Manish Kumar Goyal[a,b,*]

[a] Department of Civil Engineering, Indian Institute of Technology Guwahati, 781039, India
[b] Discipline of Civil Engineering, Indian Institute of Technology Indore, 453552, India

ARTICLE INFO

*Keywords:*
Droughts
Ecohydrological resilience
Ecosystem water use efficiency
Evapotranspiration
Hydroclimatic disturbances
Net primary productivity

ABSTRACT

The carbon and water cycles play an important role in ecosystem functioning and are linked to each other through different physical and biological processes. The hydroclimatic disturbances such as droughts affect both hydrological as well as the ecological processes. Increasing hydroclimatic disturbances under climate change will adversely affect the ecohydrological processes and hence, the assessment of the ecohydrological resilience and its controlling factors is important for the sustainability of the ecosystems. In this study, an assessment of the resilience of terrestrial ecosystems in India to hydroclimatic disturbances was carried out at the district (i.e. administrative division) scale. Ecosystem water use efficiency ($WUE_e$), defined as the ratio of net primary productivity (NPP) to evapotranspiration, was used as an indicator of ecosystem functioning or its response to hydroclimatic disturbances. We found a large spatial variation in $WUE_e$ in India at district scale, which was significantly higher in lower Himalayan regions compared to rest of the country. Increasing trend in $WUE_e$ was found for central parts of the country. The resilience was measured in terms of the ratio of the $WUE_e$ under the dry conditions and the mean $WUE_e$, which indicates the ability to absorb hydroclimatic disturbance. Out of 634 districts considered for this study, only 241 (~38%) districts were found resilient to dry conditions, whereas a significant reduction in $WUE_e$ was observed for some of the districts. The resilience at district scale indicates the cross-biomes response of ecosystems. In general, the forest dominated districts had higher resilience compared to districts dominated by other biome types. Also, districts having temperate climate were found having higher resilience. Out of 30 states and union territories (UTs) only 10 states had more than 50% resilient area. The results of this study highlight the need for better ecosystem management policies in the country.

## 1. Introduction

The concept of resilience, introduced by Holling (1973), has emerged immensely over last few decades (Folke, 2016). Resilience is defined as the ability of a system to maintain its structure and patterns of behavior in the face of disturbance (Holling, 1986). Resilience is having the capacity to persist in the face of change, to continue to develop with ever-changing environments (Folke, 2016). Simply, it relates to the capacity of a system to recover after being hit by some disturbance (Walker and Salt, 2013). It quantifies the capacity of a system to adapt or even transform into new development pathways under the dynamic change. The resilience approach is perceived as a subset of sustainability science by many (Anderies et al., 2013; Walker and Salt, 2006). Resilience cannot be defined in terms of a single measurement or number; rather, it is defined based on a set of attributes (Walker and Salt, 2013). To assess the resilience of the system, the identity (a measure of system's response/functioning) of a system needs to be identified first. The resilience analysis focuses on how that identity might be changing over time, and what threatens that identity (Walker and Salt, 2013).

The change in the Earth's climate due to increase in the greenhouse gas and aerosol concentrations in the atmosphere is leading to the higher occurrence of the extreme hydroclimatic disturbances such as droughts and heat waves (Dale et al., 2000; Karl and Trenberth, 2014; Meehl and Tebaldi, 2004; Wheeler and Braun, 2013), which affects the ecosystem functioning (Breshears et al., 2005; Dale et al., 2000; Thomey et al., 2011; Xu et al., 2017; Zhao and Running, 2010). Climate change is influencing the cloud formation mechanisms, precipitation, and runoff patterns in India (Gosain et al., 2006; Mishra et al., 2016; Mishra and Lilhare, 2016). The productivity of terrestrial ecosystems is adversely affected by such hydroclimatic disturbances. Terrestrial ecosystems play an important role in global carbon cycle as a major sink

* Corresponding author at: Discipline of Civil Engineering, Indian Institute of Technology Indore, 453552, India.
*E-mail address:* vipmkgoyal@gmail.com (M.K. Goyal).

https://doi.org/10.1016/j.jhydrol.2018.07.079

Available online 31 July 2018

for atmospheric $CO_2$ (Cao and Woodward, 1998; Ciais et al., 1995; Yu et al., 2014). Terrestrial plants consume $CO_2$ from the atmosphere during photosynthesis and lose some water at the same time, which regulates the mass-energy exchange between the vegetation and the atmosphere (Keenan et al., 2013).

In order to assess the resilience of the ecosystem, researchers use indices that represent the system behavior or the identity (Fiering, 1982a,b). Here, we used ecosystem water use efficiency ($WUE_e$) to assess the terrestrial ecosystem's response to hydro-climatic disturbances. $WUE_e$ represents the coupling of carbon and water cycles and is defined as the ratio of the rate of carbon uptake and the water loss (Ponce Campos et al., 2013; Song et al., 2017; Tang et al., 2014). It links the biological and physical processes over the land surface, which makes it suitable to understand the response of ecosystem productivity to climatic changes (Huang et al., 2017). The hydroclimatic conditions play a crucial role in the spatiotemporal variation of $WUE_e$ by affecting the ecosystem evaporation, transpiration and carbon uptake (Niu et al., 2011; Yang et al., 2016). The hydroclimatic disturbances such as droughts and heat waves lead to lesser precipitation along with the change (increase or decrease) in the evapotranspiration. This alters the hydrologic balance and the water availability, which affects the ecosystem productivity. $WUE_e$ has been widely used to determine the ecosystem's response to hydroclimatic disturbances (Ponce Campos et al., 2013; Sharma and Goyal, 2018; Zhang et al., 2014). However, recent studies have investigated the response of $WUE_e$ to drought at global or regional scales (Huang et al., 2017; Yang et al., 2016). There is a contrast in the response of $WUE_e$ to droughts for different biomes around the world. In general, different biomes have differences in correlation between $WUE_e$ and drought indices (Huang et al., 2017). Generally, the water use efficiency (WUE) is defined in different ways in the literature based on the different indicators of carbon uptake and at different scales such as leaf, canopy, and ecosystem (Niu et al., 2011). For example, Niu et al. (2011) studied the WUE at leaf, canopy, and ecosystem levels with different indicators of carbon uptake and water loss from the ecosystem. The WUE in this study is the ecosystem water use efficiency ($WUE_e$). Different indicators used for carbon uptake include: gross primary productivity (GPP), net primary productivity (NPP), gross ecosystem productivity (GEP) and net ecosystem $CO_2$ exchange (NEE) (Huang et al., 2017; Niu et al., 2011; Ponce Campos et al., 2013; Sharma and Goyal, 2018; Tang et al., 2014; Xue et al., 2015; Yang et al., 2016). However, NPP is the most widely used indicator of ecosystem carbon uptake (Huang et al., 2017; Zhang et al., 2014) and hence, was used in the present study. NPP is defined as the difference between the plant photosynthesis and the autotrophic respiration (Roxburgh et al., 2005). NPP is an effective indicator of ecosystem functioning and carbon fluxes from ecological and physiological processes (Cao and Woodward, 1998). As an indicator of water loss from the ecosystem, evapotranspiration (ET) is widely used (Ponce Campos et al., 2013). For this study, we defined $WUE_e$ as the ratio of NPP to ET. Ponce Campos et al. (2013) assessed the resilience of ecosystems in North America and Australia to the early twenty-first-century drought through enhanced $WUE_e$ in the water-limited period. The resilient ecosystem sustains its productivity to by increasing or maintaining cross-biome $WUE_e$ during the hydroclimatic disturbance. A similar analysis was carried out by Sharma and Goyal (2018) at river basin scale in India, which indicated that a large part of the country was not resilient to such disturbances. However, the study was conducted at very coarse resolution (i.e. river basins). Considering the large size of country and spatial variation in the controlling factors (i.e., land cover and climate), a detailed (i.e. higher resolution) examination of ecohydrological resilience is required for better understanding of the process. Therefore, in this study, we compared the functional response of ecosystems (in terms of the change in cross-biome $WUE_e$) in different parts of India to hydroclimatic disturbances at the district scale. The districts are the administrative or political divisions within the states in India. The district-level response of terrestrial ecosystems to drought represents the combined responses of different biomes and climates present in the districts. The objectives of this study were: (1) To assess the spatiotemporal pattern of $WUE_e$ at the district level in India, (2) To evaluate the district level ecohydrological resilience to hydroclimatic disturbances (i.e. drought), and (3) To evaluate the role of controlling factors (i.e. climate and biome types) in ecohydrological resilience at district scale. Due to lack of ground measurements and eddy covariance sites in India, the remote sensing based NPP (MOD17A3) and ET (MOD16A3) products from the NASA Earth Observation System (EOS) program were used. These products have been validated and used in different global and regional studies (Anav et al., 2015; Turner et al., 2006; Xue et al., 2015; Zhao and Running, 2010).

## 2. Materials and methods

### 2.1. Study area

The present study was conducted at district and state levels in India. Districts represent the administrative divisions within the states in India. There are a total of 29 states and 7 union territories (UTs) in India. Out of these, we considered a total of 30 states and UTs for this study, which include all state and one UT, namely Delhi. As per 2011 Census of India, there are a total of 640 districts. We considered 634 districts leaving those having no valid pixels of MODIS NPP and ET raster and those on islands. There is a large variation in the area of districts ranging from 9 $km^2$ (Mahe in the state of Puducherry) and 45652 $km^2$ (Kachchh in the state of Gujarat). Mahe was not included in this study.

### 2.2. MODIS NPP and ET

We used the global annual MOD17A3 (NPP) and MOD16A3 (ET) products from the NASA Earth Observation System (EOS) program. The global datasets were developed by Numerical Terradynamic Simulation Group (NTSG) at University of Montana (UMT) (available from http://www.ntsg.umt.edu/). The MOD17A3 and MOD16A3 products were generated using the MOD17 algorithm (Running et al., 2004; Zhao et al., 2005) and improved MOD16 algorithm (Mu et al., 2007, 2011, 2013), respectively. These datasets were available from 2000 to 2014 at a spatial resolution of 1 km. The MOD17 algorithm is based on the radiation use efficiency procedure of Monteith (1972). The algorithm considers that the productivity of vegetation under well-watered and fertilized conditions is linearly related to the amount of Absorbed Photosynthetically Active Radiation (APAR). A conversion efficiency parameter ($\varepsilon$) is used to convert APAR to actual productivity estimated. The parameter $\varepsilon$ varies for vegetation types and climate conditions. To calculate NPP, MOD17 also estimates daily leaf and fine root maintenance respiration, annual growth respiration, and annual maintenance respiration of live cells in woody tissue. MOD17 user guide provides further details of the algorithm and is available at http://www.ntsg.umt.edu/files/modis/MOD17UsersGuide2015_v3.pdf. The MODIS NPP dataset has been validated and used in many studies (Turner et al., 2006; Zhao et al., 2005, 2006). The MOD 16 algorithm is based on the improved ET algorithm of Mu et al. (2011), which uses Penman-Monteith equation. The ET includes evaporation from wet and moist soil, from rain water intercepted by the canopy before it reaches the ground, and the transpiration through stomata on plant leaves and stems. The remote sensing data from MODIS provides input for surface biophysical variables affecting ET, including albedo, biome type and leaf area index (LAI). The detailed algorithm of MOD16 is available at http://www.ntsg.umt.edu/project/modis/mod16.php. This global ET product was validated by Mu et al. (2011) using 46 eddy flux towers dataset and it was found that the dataset can be used to estimate actual ET with satisfactory accuracy in Asia. Previous studies in India used MOD16 ET as an estimate of actual ET (e.g. Shah and Mishra, 2016). Due to the lack of ground measurements, it was not possible for the

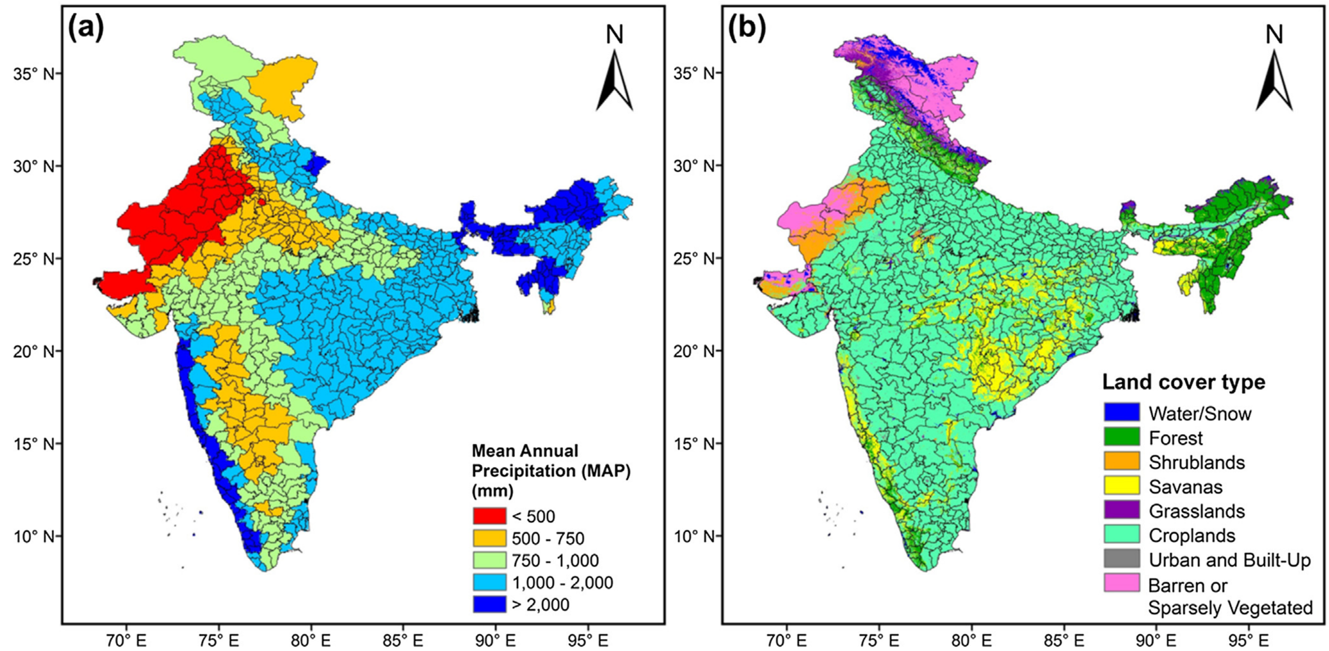


**Fig. 1.** Spatial variation of (a) district level mean annual precipitation (MAP) for the duration 2000–2014 and (b) land cover types in India. Districts are the administrative divisions within the states in India. MAP was calculated using 0.25° × 0.25° gridded precipitation data for Indian Meteorological Department (IMD).

authors to validate these products.

### 2.3. Precipitation and drought index

Daily gridded rainfall dataset (IMD4) from Indian Meteorological Department (IMD) at a high spatial resolution (0.25° × 0.25°) was used in this study (Pai et al., 2014). The dataset is prepared from daily rainfall records from 6955 rain gauge stations in India and is available from 1901 to 2015. The total annual precipitation (sum of daily precipitation, mm/year) and mean annual precipitation, MAP, (mean of annual precipitation, mm/year) at same resolution was computed from daily values. The district level MAP for the duration 2000 to 2014 is shown in Fig. 1(a). To identify the drought condition, we used Palmer Drought Severity Index (PDSI). The monthly PDSI dataset was obtained from Dai and NCAR (2017) at monthly timescale. PDSI is a measure of dryness, which is computed based on the precipitation and temperature. It is a standardized index and its value ranges from -10 to +10. The negative values of PDSI indicate the dry conditions, whereas the positive values indicate the wet conditions. Further details of PDSI and drought classifications based on PDSI can be found at http://droughtmonitor.unl.edu/AboutUSDM/DroughtClassification.aspx.

### 2.4. Land cover data

The land cover classification used in this study is based on 10 years (2001–2010) of Collection 5.1 MCD12Q1 land cover type data and was obtained from the USGS Land Cover Institute (LCI, https://landcover.usgs.gov/global_climatology.php) (Broxton et al., 2014). Croplands (CR) is the most dominant land cover type in India, covering about 50% of the total geographical area. This dataset has 17 different classes of land cover types. The previous study for the region (i.e., India) reported that different forest classes or cropland classes had nearly same values of $WUE_e$ (Sharma and Goyal, 2018). For example, Sharma and Goyal (2018) showed that the $WUE_e$ value for all forest classes was nearly same (~0.95 $gC\,m^{-2}\,mm^{-1}$). Among five forest classes, only Deciduous Broadleaf Forest (DBF) had lesser values, but it covers only 0.56% of the area in India. Similarly, the value of resilience index ($R_d$, defined in the next section) was also nearly the same for different forest types except for DBF. Likewise, crop classes also had similar behavior. Therefore, we reclassified the land cover map to reduce the number of classes by merging similar classes. For example, Evergreen Needleleaf Forest, Evergreen Broadleaf Forest, Deciduous Needle leaf Forest, Deciduous Broadleaf Forest and Mixed Forests were considered as a single forest class. Croplands and Cropland/Natural Vegetation Mosaic were merged to a single cropland class. Closed Shrublands and Open Shrublands were merged to form Shrublands class. Similarly, Savannas and Water/Snow classes were formed by merging similar classes of MCD12Q1 land cover type. Fig. 1(b) shows the distribution of different land cover types (i.e. the classes used in this study) in India. To estimate the potential role of vegetation type on $WUE_e$, average $WUE_e$ was calculated for districts dominated by different land covers. A threshold of 40% was taken to determine the dominance of a land cover in a district.

### 2.5. Calculation of ecosystem water use efficiency ($WUE_e$)

Annual $WUE_e$ rasters were prepared using MODIS NPP and ET rasters. Only valid and non-fill values of NPP and ET rasters were considered for the calculation. Average NPP and ET were computed for every district by taking the average of all pixel values in the district. The district-scale $WUE_e$ was calculated as the ratio of NPP and ET. Mean annual $WUE_e$ was computed as the average of 15 years (2000–2014) annual $WUE_e$ for every district.

### 2.6. Resilience analysis

The resilience analysis was carried out using $WUE_e$ as the indicator of ecosystem's response to hydroclimatic disturbance (Ponce Campos et al., 2013; Sharma and Goyal, 2018). Water-limited condition (i.e. drought) was identified based on PDSI. Initially, the driest year was chosen for every district based on the annual precipitation for the district. The water-limited condition (i.e. drought condition) in that year was validated based on the values of PDSI for the year. We calculated the resilience index ($R_d$) for every district (Sharma and Goyal, 2018). $R_d$ was defined as the ratio of the $WUE_e$ in the driest year (termed as $WUE_d$) to the mean annual value of $WUE_e$ (termed as $WUE_m$). The response of $WUE_e$ at district scale is used to assess its resilience. As a district may contain different climate types or biomes; hence our objective was to assess the response of cross-biome $WUE_e$ at district scale

rather than for individual biome or climate type. Considering the contrast in the response for different biomes or climates, we further related to district level resilience to dominating biome or climate types. $R_d$ is dimensionless and it can be used to compare the resilience characteristics of different regions. Any district having the value $R_d$ greater than or equal to unity was considered as resilient. Similar to Sharma and Goyal (2018), the non-resilient ecosystems were further classified into three categories. For $0.9 \le R_d < 1$, the ecosystem was termed as slightly non-resilient. For $0.8 \le R_d < 0.9$, the ecosystem was termed as moderately non-resilient. For $R_d < 0.8$, the ecosystem was termed as severely non-resilient.

### 2.7. Trend analysis of $WUE_e$

To examine the temporal variation in the $WUE_e$, a linear trend analysis was carried out at the district scale. The statistical significance of trend was evaluated based on non-parametric Mann Kendall (MK) trend test (Kendall, 1975; Mann, 1945) at 5% significance level. MK trend test is widely used in the field of hydrology.

## 3. Results and discussions

The spatial variations of district-level MODIS NPP and ET are shown in Fig. 2, which is the average over the period 2000–2014. Both NPP and ET had large spatial variation over the country. The northeast and the Western Ghats had higher NPP and ET compared to the remaining country, which can mainly be attributed to the higher precipitation and the presence of forests in these regions (see Fig. 1). The agricultural lands of Indo-Gangetic plains (i.e., the north part of the country) had moderate NPP ranging between 500 and 1000 gC m$^{-2}$. The lower Himalayan regions in the north had moderate NPP (ranging between 400 and 900 gC m$^{-2}$), whereas the region had lesser ET (ranging between 300 and 600 mm). The arid and semi-arid regions in the west had least NPP. These regions receive very less annual precipitation and have very sparse vegetation. Some regions in the north (e.g. upper parts of Jammu and Kashmir (JK), see Fig. 9) also had very less NPP. The spatial pattern of MODIS NPP is partly consistent with the Carnegie–Ames–Stanford Approach (CASA) model simulated NPP over the period 1981 to 2005 (Nayak et al., 2013).

Fig. 3 shows the spatial pattern of mean annual $WUE_e$ ($WUE_m$) at district scale in India for the period 2000–2014. Due to the large variation in the controlling factors such as precipitation, temperature, and solar radiation, $WUE_e$ showed a large spatial variation across the country. The district level $WUE_m$ ranged between 0 and 2.19 gC m$^{-2}$ mm$^{-1}$. Higher $WUE_m$ was found in the northeast and lower Himalayan regions. In northeast India, the higher $WUE_m$ can mainly be attributed to the higher NPP due to the presence of the forest (Sharma and Goyal, 2018). Western Ghats had higher NPP (Fig. 2a) but showed lesser $WUE_m$, which is due to high rate of ET (Fig. 2b).

Fig. 4 shows the distribution of linear trend for districts across the country. Decreasing trend was found for districts along the lower Himalayan regions in the north and northeast India. These regions had higher $WUE_e$ (see Fig. 3). Significant increasing trend (as per MK test) of magnitude > 0.01 gC m$^{-2}$ mm$^{-1}$ yr$^{-1}$ was observed for central India. This region had moderate $WUE_e$. In general, regions with higher $WUE_e$ showed decreasing trend, whereas the regions with lesser $WUE_e$ showed increasing trend. However, there were very few districts with the significant decreasing trend (only 10 districts). About 68% of the districts had increasing trend (only 22% were significant), whereas the remaining districts had decreasing trend (only 1.6% were significant).

NPP and $WUE_e$ are dependent on the vegetation types as different vegetation types have variations in carbon uptake and water consumption. Fig. 5 shows the average $WUE_m$ for districts dominated by different land covers (i.e., vegetation types). Forest dominated districts had the highest $WUE_e$, which is consistent with other studies (Sharma and Goyal, 2018; Tang et al., 2014). This explains the higher $WUE_e$ in northeast India. It should be noted that the average $WUE_e$ is the average of annual $WUE_e$ of the districts dominated by a particular land cover, not the average for that land cover as the district dominated by one land cover also has other land covers. The previous study has also reported higher $WUE_e$ for these land cover types in India (Sharma and Goyal, 2018). The average $WUE_e$ for Evergreen Needleleaf Forest (ENF), Evergreen Broadleaf Forest (EBF), Deciduous Broadleaf Forest (DBF), and Mixed Forests (MF) in India were 0.959, 0.948, 0.416, and 1.087 gC m$^{-2}$ mm$^{-1}$, respectively (Sharma and Goyal, 2018). We found average $WUE_e$ for forest dominated districts as 1.00 gC m$^{-2}$ mm$^{-1}$, which is close to the values for individual forest classes. The average $WUE_e$ for Grasslands (GR) was 0.488 gC m$^{-2}$ mm$^{-1}$, (Sharma and

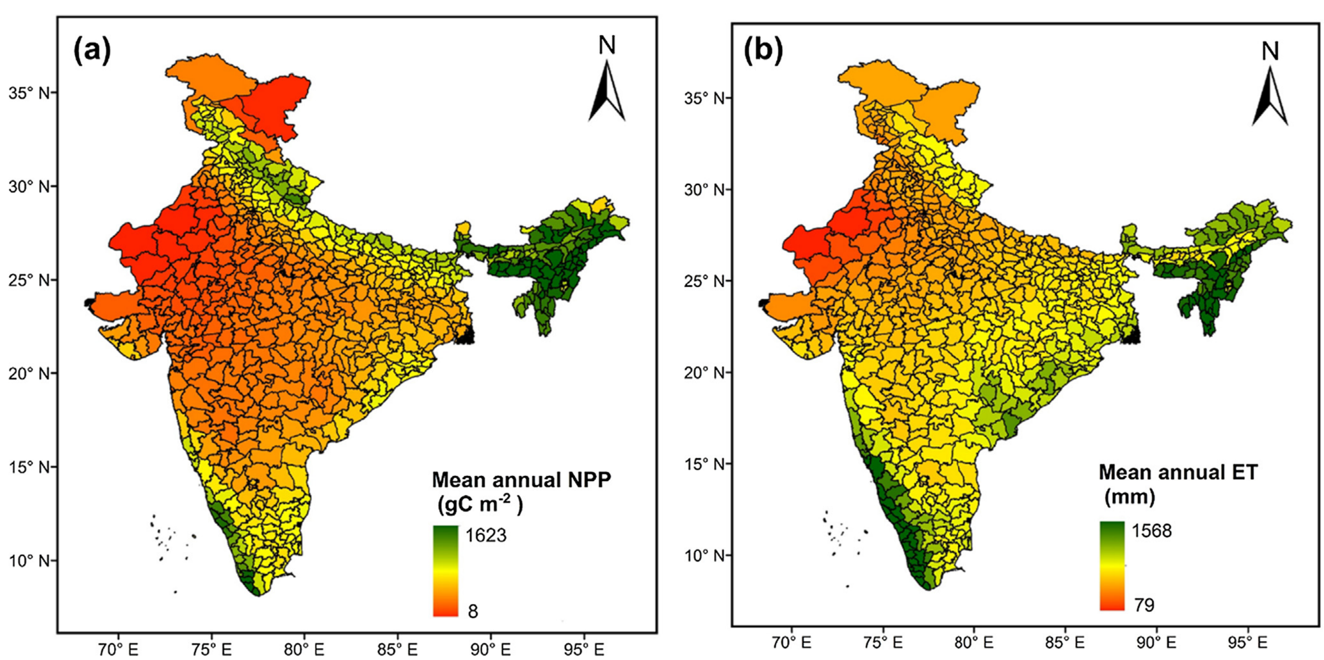


**Fig. 2.** District-level mean annual MODIS (a) NPP and (b) ET in India for the duration 2000–2014. Northeast and the Western Ghats had higher NPP and ET due to higher precipitation and presence of forests.

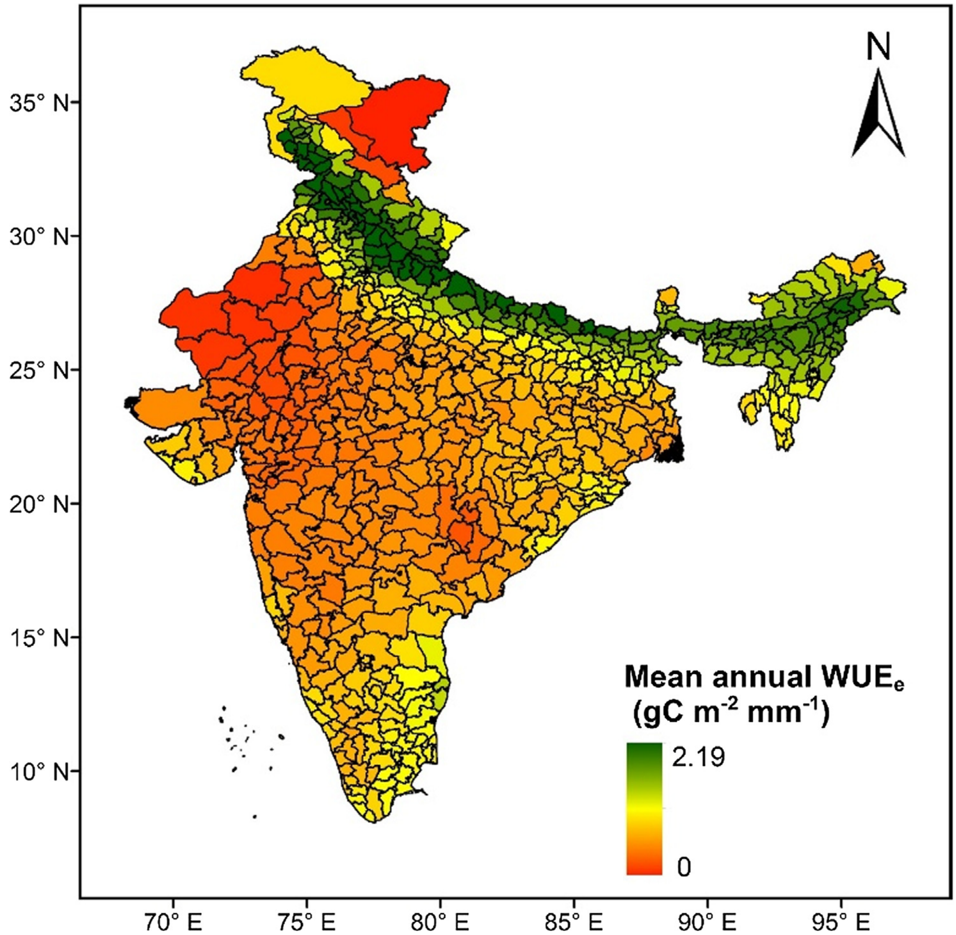


**Fig. 3.** Mean annual ecosystem water use efficiency ($WUE_e$) at district scale in India. Annual $WUE_e$ was computed as the ratio of annual NPP and ET. The districts in the lower Himalayan region had higher $WUE_e$ compared to rest of the country, whereas the arid regions in the west had least $WUE_e$.

Goyal, 2018) whereas the average $WUE_e$ for the GR dominated districts found was 0.77 $gC\,m^{-2}\,mm^{-1}$. The average $WUE_e$ for Cropland (CR) and Cropland/Natural Vegetation Mosaic (CNV) were 0.619 and 0.689 $gC\,m^{-2}\,mm^{-1}$, whereas the average $WUE_e$ for the cropland dominated districts was 0.72 $gC\,m^{-2}\,mm^{-1}$. Similarly, average $WUE_e$ for the Shrubland, Savanas and Baren land dominated districts were 0.17, 0.54 and 0.19 $gC\,m^{-2}\,mm^{-1}$. This indicates that the $WUE_e$ of districts dominated by a particular vegetation type was related to $WUE_e$ of the corresponding vegetation types. Though, there were differences in the values of $WUE_e$, which was due to the presence of different vegetation types with in the district.

Annual PDSI was computed for every district in India for the study duration. Fig. 6 shows the values of PDSI for every district in their respective driest years. It is clear from the figure that most parts (600/634 districts) of the country experienced drought conditions (PDSI $< -1$) during their respective driest year, which accounts for about 94.64% of the districts. Only 34 districts had value of PDSI greater than $-1$ but less than 0, which also represent below average precipitation conditions. Out of 634 districts, 501 districts had moderate to exceptional drought conditions (i.e., PDSI $< -2$). Fig. 7 shows the results of the district level resilience analysis. $R_d$ was calculated based on the mean and driest year values of $WUE_e$ as discussed in the methodology. Out of 634 districts considered for this study, we found that 241 ($\sim$38%) districts were resilient. Remaining 62% districts were found non-resilient under different classes of non-resilience. The number of districts with slightly, moderately and severely non-resilient was 180 ($\sim$28.4%), 80 ($\sim$12.6%) and 133 ($\sim$21%), respectively. In terms of area under different classes, we found that the resilient, slightly, moderately and severely non-resilient classes covered 31.65%, 27.51%, 11.52%, and 29.32%, respectively, of area of the country. This indicates the around 68% of area was not resilient. Most of the districts in the northeast and north India were either resilient or slightly non-resilient. The arid or semi-arid regions in the west were non-resilient. Some parts of eastern states were also found non-resilient. Fig. 8(a) shows the distribution of number of districts for ranges of $R_d$. Most of the districts are falling either in resilient or slightly non-resilient classes. The range 0.9–1.0 holds most number of districts (=180). Also, around 63% of the districts fall in the range of 0.8–1.1, this shows that only 37% of the stations had shown clear characteristics of either resilient or non-resilient. Recent studies have shown that different biomes had a tendency to increase its $WUE_e$ under water stress conditions (Huang et al., 2017; Liu et al., 2015), therefore, we performed a correlation analysis between the ratio of driest year precipitation to mean precipitation and the $R_d$ (Fig. 8b). The Pearson's correlation was found 0.125, indicating no dependencies between these two variables. This shows that the behavior of $WUE_e$ was not controlled only by the precipitation, but it also represents other ecohydrological processes.

There are different factors that affect the ecosystem functioning including climatic factors such as precipitation, temperature and solar radiation, and biome types. In order to find out the factor controlling the ecohydrological resilience, we analyzed the contribution of different biome types and climate types. There was a significant difference (p-value $< 0.05$) in the average $R_d$ value for different biomes and climate types. The average $R_d$ for forest, shrubland, savannas, grassland, cropland and barren land dominated districts were 0.99, 0.28, 0.83, 0.98, 0.92 and 0.77, respectively, which shows that biome type doesn't completely relate to resilience. However, the forest class showed higher resilience compared to other biomes. We found that there were about

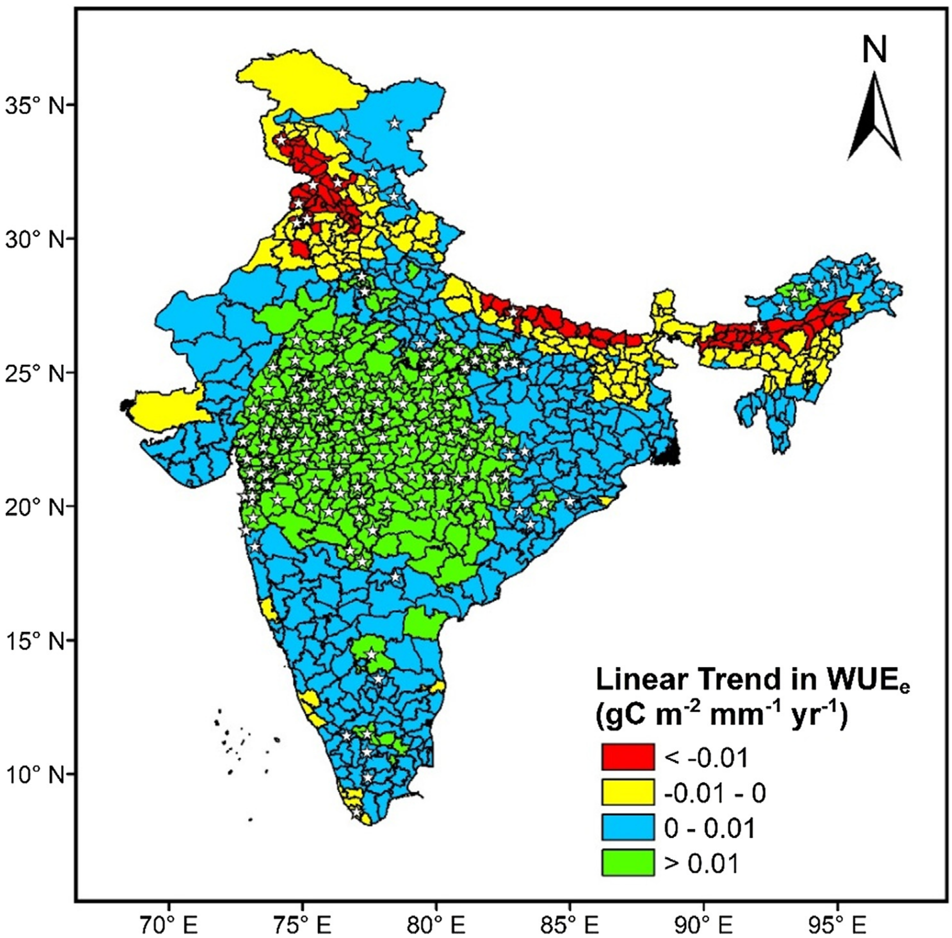


**Fig. 4.** The linear trend analysis of district-level $WUE_e$. Star symbol (white) represents the district with the statistically significant trend at 5% significance level. Out of 634 districts, only 22% had significant increasing trend (mostly in central regions) and only 1.6% had significant decreasing trend. The regions with high $WUE_e$ (i.e., the lower Himalayan regions, see Fig. 3) had decreasing trend.

75 districts with forest cover greater than 40% of district area. Out of these districts, more than 50% were resilient. Whereas, about 65% of the districts with less than 20% forest cover were not resilient. This also indicates the higher resilience of forest dominated districts. It can also be seen that the forest dominated area in northeast and north India are mostly resilient, which is consistent with the findings of Sharma and Goyal (2018). The $R_d$ values for Evergreen Needleleaf Forest (ENF), Evergreen Broadleaf Forest (EBF), Deciduous Broadleaf Forest (DBF), and Mixed Forests (MF) were 1.03, 1.00, 0.70, and 0.95, respectively (Sharma and Goyal, 2018). The $R_d$ value for different forest classes was close to that for forest dominated districts. On the other hand, the only 35% of cropland dominated districts were found resilient. The $R_d$ values for Cropland (CR) and Cropland/Natural Vegetation Mosaic (CNV) were 0.98 and 0.97, whereas the cropland dominated districts had slightly lesser $R_d$ value (= 0.92). It should be noted that croplands cover more than 50% area in India. The $R_d$ value for Grasslands (GR) was 0.98, which is equal to the average $R_d$ value for the grassland dominated districts. To take into account the effect of different climate types, we used Koppen-Geiger climate classification maps from Kottek et al. (2006). Koppen-Geiger climate classes A (Tropical), B (Dry) and C (Temperate) cover about 30%, 20% and 48% of the country's districts respectively. The average $R_d$ for district dominated these classes was

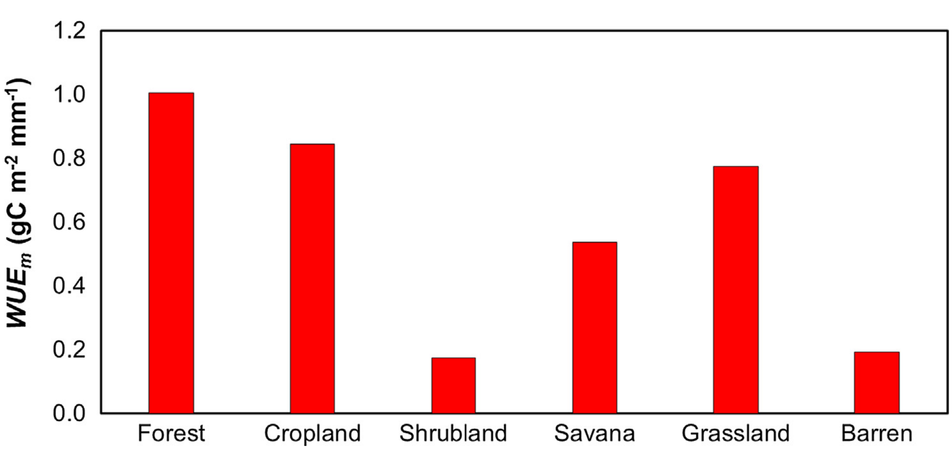


**Fig. 5.** Average $WUE_m$ for districts dominated by different land covers. A district with more than 40% of a particular land cover was considered dominated by that land cover.

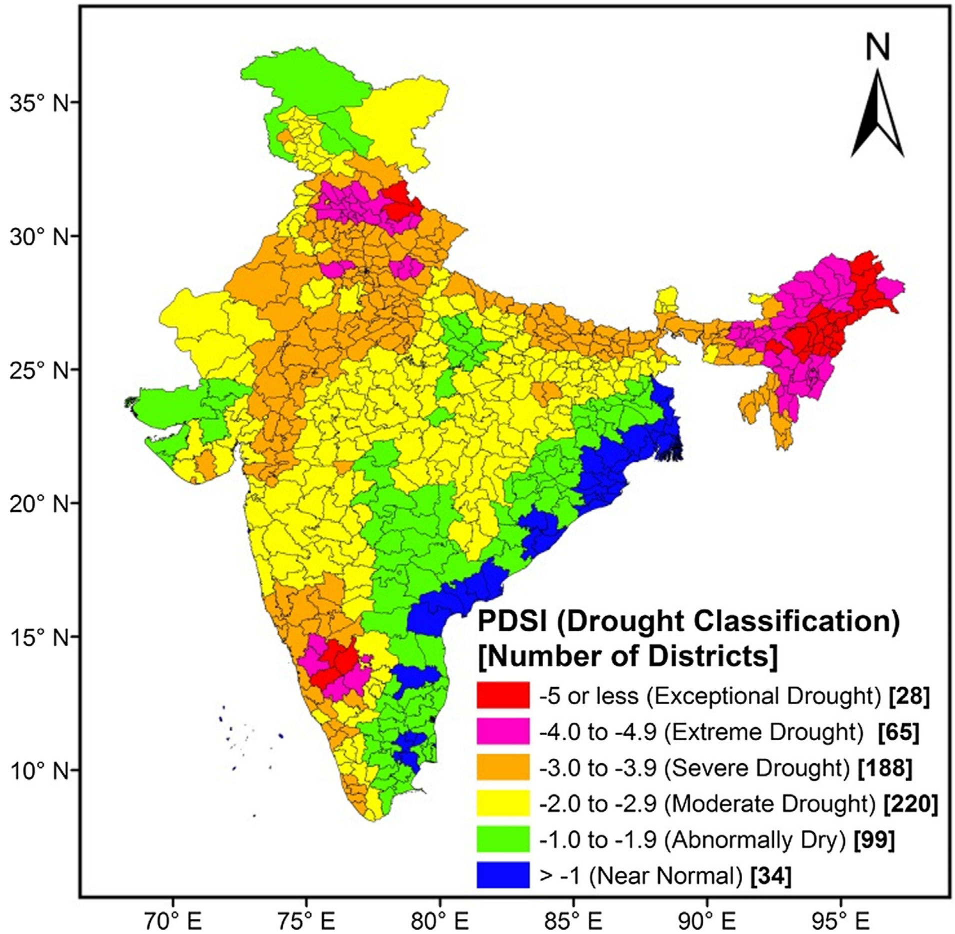


**Fig. 6.** Map showing the Palmer Drought Severity Index (PDSI) values and drought classification for every district during the respective driest years in the study duration. Numbers in the square brackets ([ ]) represent the number of districts having respective drought class.

0.89, 0.89, and 0.9, respectively. The percent of districts under these climates that were found resilient are 32%, 38% and 42%, respectively. This shows that districts in the temperate climate had higher tendency to be resilient, which is also consistent with the findings of Sharma and Goyal (2018). The average $R_d$ values for A, B and C climate types were 0.818, 0.787, and 1.02, respectively, which also indicates that climate type C was more resilient. However, similar to the biome types, the resilience at district level does not completely relate to climate type. There are resilient districts with land cover and climates that were found less resilient. Some global studies showed that different biomes had contrasting responses to droughts (Huang et al., 2017; Yang et al., 2016). Our district-level results are not completely consistent with these studies for the reason that there are multiple vegetation types within the geographical area of a district. For example, within a district we can have forest as well croplands. The district level response of $WUE_e$ is the combined response of multiple biomes/climates rather than that of a single biome/climate. We identified some relation between these controlling factors and the resilience, but there is still need of more observation and research to identify the other eco-hydrological factors controlling the resilience.

In addition to district-level resilience assessment, we also examined the resilience at state scale. Fig. 9 shows the percentage of resilient area in every state. The percentage of resilient area was computed using sum of areas of resilient districts and total area of state. Sikkim (SK) was the only state with 100% resilient area. All four districts in the state were found resilient. Two states namely Rajasthan (RJ) and Chhattisgarh (CH) had 0% resilient area. RJ is located in the western arid regions and has very less vegetation. It should be noted that all three classes of non-resilience were considered non-resilient. These states had districts with different classes of non-resilience, but did not have a single resilient district. Out of 30 states and UTs considered, only 10 had more than 50% resilient area. In general, it was found that the states in the lower Himalayan regions had higher resilient areas (in terms of percent of total state area), for example, Sikkim (SK, 100%), Punjab (PB, 88.11%), Haryana (HR, 76.02%), Uttarakhand (UK, 75.26%), Himachal Pradesh (HP, 73.19%), and Arunachal Pradesh (AR, 64.04%). In the south, Tamil Nadu (TN, 56.74%) was the most resilient followed by Andhra Pradesh (AP, 53.43%) and Telangana (TL, 48.61%). Whereas, Karnataka (KR, 17.38%) and Kerala (KL, 19.13%) had the minimum percentage of resilient area in south. Among northeastern states, Assam (AS, 20.72%) had the minimum percentage of resilient area.

Our study highlights the resilience of the terrestrial ecosystems in different parts of India at state and district scale. India is a developing nation, which has been expanding its infrastructure exponentially. Economic growth in India requires rapid industrialization and infrastructure development. The infrastructural and economic developments come at the cost of damage to natural ecosystems. Anthropogenic activities such as land use and land cover alterations, deforestation, and urbanization affect the ecological process and primary production. Every state in India has shown a consistent increase in Gross State Domestic Product (GSDP), which indicates that continuous development occurring in different sectors. On the other hand, increase in the extreme hydroclimatic events in India has increasingly been reported (Mallya et al., 2015; Roxy et al., 2017; Sharma and Mujumdar, 2017). The ongoing climatic changes may lead to more extreme hydroclimatic events, which will put tremendous pressure on terrestrial ecosystems to

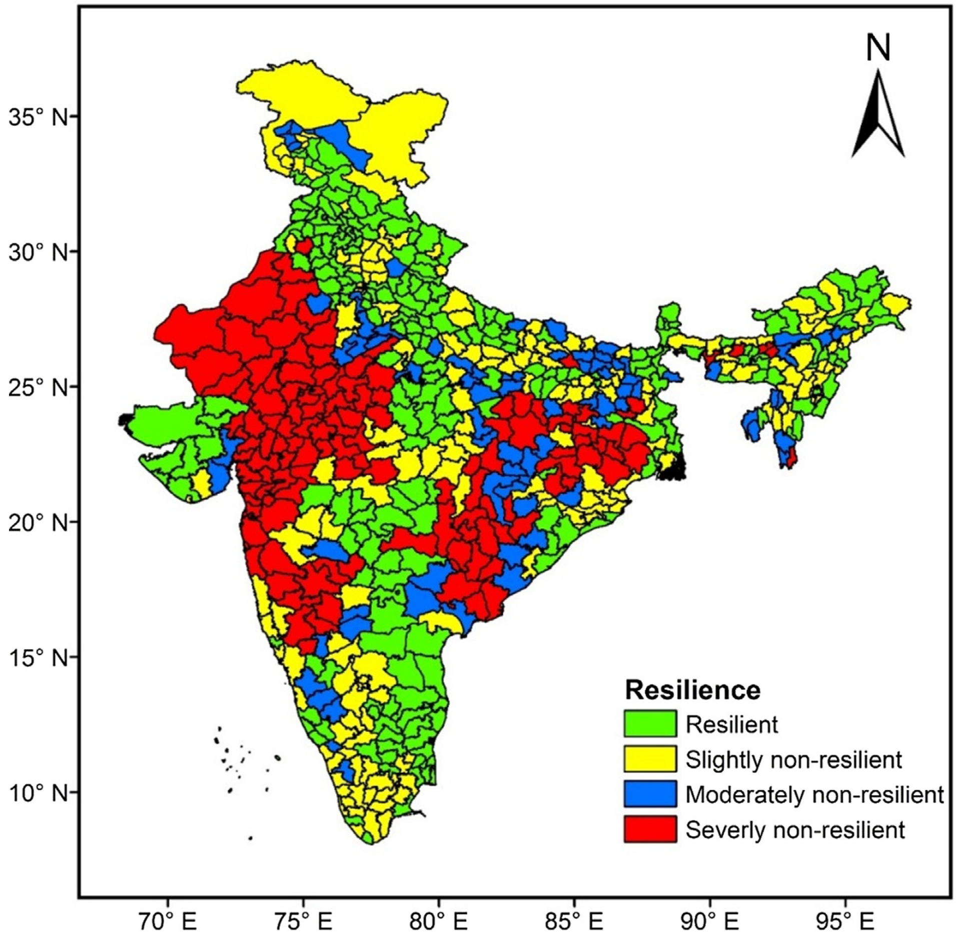


**Fig. 7.** Map showing the resilience of different districts in India. The resilience was assessed in terms value of $R_d$, which represent the ratio of $WUE_e$ during the driest year ($WUE_d$) and the mean $WUE_e$ ($WUE_m$).

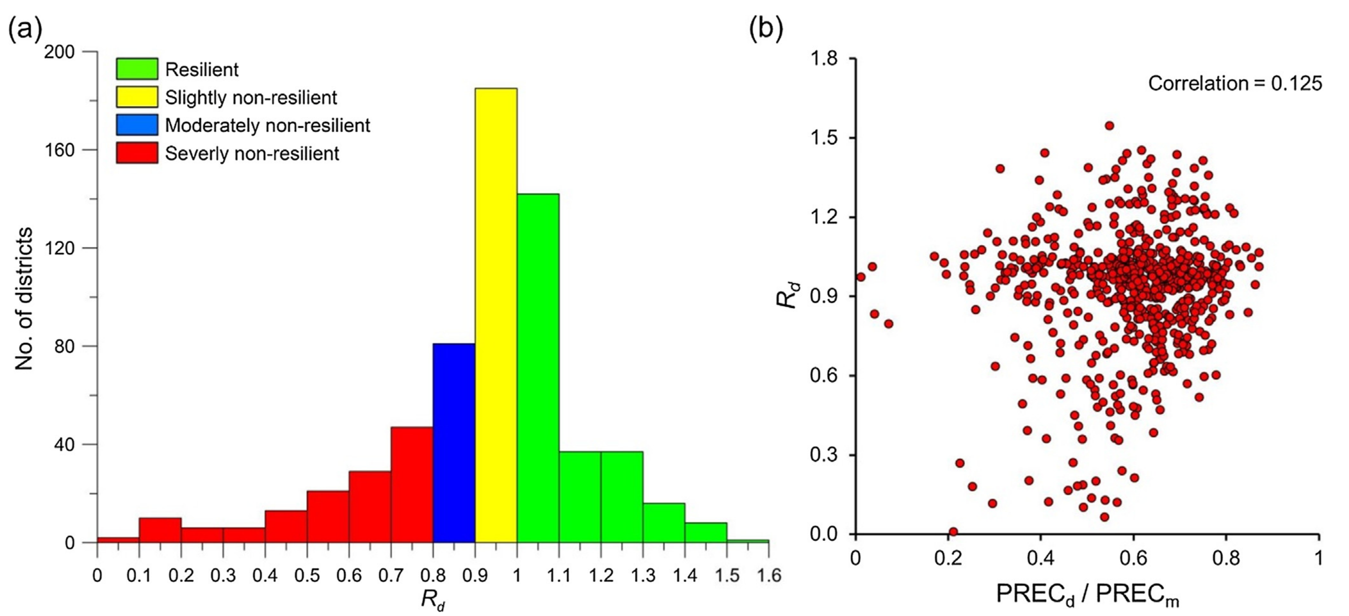


**Fig. 8.** Number of districts for different ranges of $R_d$ (the ratio of driest year $WUE_e$ to mean $WUE_e$) (a) and scatter plot between $R_d$ and $PREC_d/PREC_m$. $PREC_d$ is the precipitation for the driest year and $PREC_m$ is the mean precipitation.

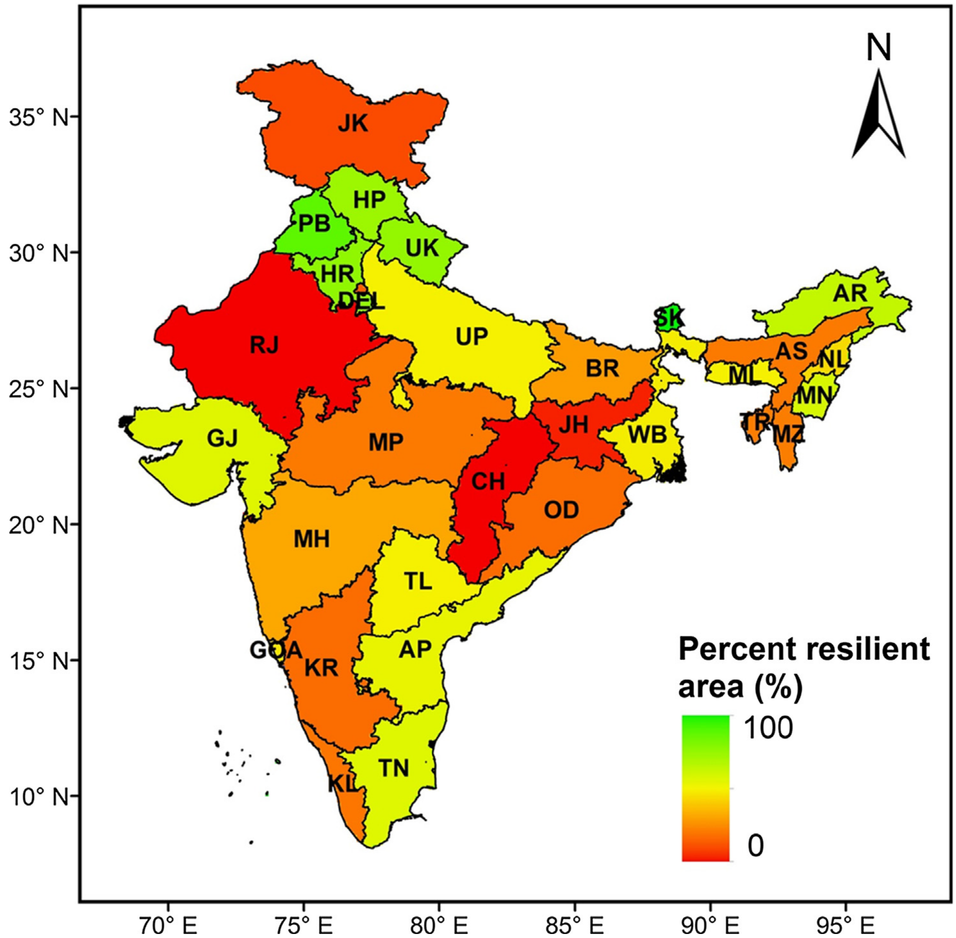


**Fig. 9.** Map showing the percentage of resilient area in each state. The resilient area is the total area of all resilient districts within the state. All the 29 states and one UT, Delhi, were considered in this study.

maintain its functioning and productivity. The reduction in primary productivity under dry condition, as found in this study, may also lead to a risk of food shortage, as both population and demand for food has been increasing.

## 4. Conclusions

This study presents an assessment of ecohydrological resilience of the terrestrial ecosystems in India to the hydroclimatic disturbances at the district level. The ecosystem water use efficiency ($WUE_e$), which is defined as the ratio of net primary productivity (NPP) to evapotranspiration (ET), was used as an indicator of ecosystem functioning or its response to hydroclimatic disturbances. Due to the presence of different climate and biome types in India, we found a significant variation in NPP, ET and $WUE_e$ across India. The forest dominated northeast and the Western Ghats had higher NPP, whereas the arid regions in the west had the least NPP. ET had a similar spatial variation over India. In contrast to NPP and ET, the $WUE_e$ was significantly higher for lower Himalayan regions of Indus, Ganga and Brahmaputra basins (i.e., in the northern and northeast regions). Western Ghats had lower $WUE_e$, despite having higher NPP, due to the higher ET. Increasing trend in $WUE_e$ was found in central India, whereas a non-significant decreasing trend was found for the lower Himalayan regions i.e. the regions with higher $WUE_e$. Among different biome types, districts dominated by forest cover had highest $WUE_e$ followed by cropland, grassland and savanna respectively. Based on the resilience analysis, which was carried out using driest year $WUE_e$ and mean $WUE_e$, it was found that out of 634 districts considered for this study only 241 (38%) districts were resilient to dry conditions. The terrestrial ecosystems in these districts had shown remarkable resilience in terms of maintaining their primary productivity under dry conditions by enhancing their $WUE_e$. From the comparison the resilience at state level, it was found that only 10 out of 30 states and union territories (UTs) had more than 50% resilient area. In general, it was found that forest dominated districts had higher resilience compared to other biome types. In terms of climate types, districts having temperature climate were found more resilient. This study provides detailed spatial information about terrestrial ecosystem's response to hydroclimatic disturbances in India and will be beneficial for ecosystem management and policymaking.

## Declarations of interest

None.

## Acknowledgements

The authors gratefully acknowledge the scholarship provided by the Indian Institute of Technology Guwahati, Assam, India to the first author for his PhD work. The authors are thankful to Numerical Terradynamic Simulation Group (NTSG) at University of Montana (UMT) for NPP and ET datasets, to Climate Data Guide, National Center for Atmospheric Research (NCAR) for PDSI data, and to Indian Meteorological Department (IMD) for precipitation data. The authors also acknowledge and appreciate the valuable comments and suggestions from two anonymous reviewers, which helped in improving the quality of the paper.

## References


Anav, A., Friedlingstein, P., Beer, C., Ciais, P., Harper, A., Jones, C., Murray-Tortarolo, G., Papale, D., Parazoo, N.C., Peylin, P., Piao, S., Sitch, S., Viovy, N., Wiltshire, A., Zhao, M., 2015. Spatiotemporal patterns of terrestrial gross primary production: a review. Rev. Geophys. 53, 785–818. https://doi.org/10.1002/2015RG000483.

Anderies, J.M., Folke, C., Walker, B., Ostrom, E., 2013. Aligning key concepts for global change policy: robustness, resilience, and sustainability. Ecol. Soc. 18. https://doi.org/10.5751/ES-05178-180208.

Breshears, D.D., Cobb, N.S., Rich, P.M., Price, K.P., Allen, C.D., Balice, R.G., Romme, W.H., Kastens, J.H., Floyd, M.L., Belnap, J., Anderson, J.J., Myers, O.B., Meyer, C.W., 2005. Regional vegetation die-off in response to global-change-type drought. Proc. Natl. Acad. Sci. U.S.A. 102, 15144–15148. https://doi.org/10.1073/pnas.0505734102.

Broxton, P.D., Zeng, X., Sulla-Menashe, D., Troch, P.A., 2014. A global land cover climatology using MODIS data. J. Appl. Meteorol. Climatol. 53, 1593–1605. https://doi.org/10.1175/JAMC-D-13-0270.1.

Cao, M.K., Woodward, F.I., 1998. Dynamic responses of terrestrial ecosystem carbon cycling to global climate change. Nature 393, 249–252. https://doi.org/10.1038/30460.

Ciais, P., Tans, P.P., Trolier, M., White, J.W.C., Francey, R.J., 1995. A large northern hemisphere terrestrial CO2 sink indicated by the 13C/12C ratio of atmospheric CO2. Science (80-.) 269, 1098–1102.

Dai, A., NCAR, N.C. for A.R.S., 2017. The Climate Data Guide: Palmer Drought Severity Index (PDSI) [WWW Document]. Natl. Cent. Atmos. Res. URL: https://climatedataguide.ucar.edu/climate-data/palmer-drought-severity-index-pdsi (accessed 07.12.17).

Dale, V.H., Joyce, L.A., McNulty, S., Neilson, R.P., 2000. The interplay between climate change, forests, and disturbances. Sci. Total Environ. 262, 201–204. https://doi.org/10.1016/S0048-9697(00)00522-2.

Fiering, M.B., 1982a. Estimates of resilience indices by simulation. Water Resour. Res. 18, 41–50. https://doi.org/10.1029/WR018i001p00041.

Fiering, M.B., 1982b. Alternative indices of resilience. Water Resour. Res. 18, 33–39. https://doi.org/10.1029/WR018i001p00033.

Folke, C., 2016. Resilience (Republished). Ecol. Soc. 21, 44. https://doi.org/10.5751/ES-09088-210444.

Gosain, A.K., Rao, S., Basuray, D., 2006. Climate change impact assessment on hydrology of Indian river basins. Curr. Sci. 90, 346–353.

Holling, C.S., 1973. Resilience and stability of ecological systems. Annu. Rev. Ecol. Syst. 4, 1–23.

Holling, C.S., 1986. The resilience of terrestrial ecosystems: local surprise and global change. In: Clark, W.C., Munn, R.E. (Eds.), Sustainable Development of the Biosphere. Cambridge University Press, Cambridge, UK, pp. 292–320.

Huang, L., He, B., Han, L., Liu, J., Wang, H., Chen, Z., 2017. A global examination of the response of ecosystem water-use efficiency to drought based on MODIS data. Sci. Total Environ. 601–602, 1097–1107. https://doi.org/10.1016/j.scitotenv.2017.05.084.

Karl, T.R., Trenberth, K.E., 2014. Modern global climate change. Science (80-.) 302, 1719–1723.

Keenan, T.F., Hollinger, D.Y., Bohrer, G., Dragoni, D., Munger, J.W., Schmid, H.P., Richardson, A.D., 2013. Increase in forest water-use efficiency as atmospheric carbon dioxide concentrations rise. Nature 499, 324–327. https://doi.org/10.1038/nature12291.

Kendall, M.G., 1975. Rank Correlation Methods. Griffin, London.

Kottek, M., Grieser, J., Beck, C., Rudolf, B., Rubel, F., 2006. World map of the Köppen-Geiger climate classification updated. Meteorol. Zeitschrift 15, 259–263. https://doi.org/10.1127/0941-2948/2006/0130.

Liu, Y., Xiao, J., Ju, W., Zhou, Y., Wang, S., 2015. Water use efficiency of China's terrestrial ecosystems and responses to drought. Sci. Rep. 5, 13799. https://doi.org/10.1038/srep13799.

Mallya, G., Mishra, V., Niyogi, D., Tripathi, S., Govindaraju, R.S., 2015. Trends and variability of droughts over the Indian monsoon region. Weather Clim. Extrem. 12, 43–68. https://doi.org/10.1016/j.wace.2016.01.002.

Mann, H.B., 1945. Nonparametric tests against trend. Econometrica 13, 245–259.

Meehl, G.A., Tebaldi, C., 2004. More frequent, and longer lasting heat waves in the 21st century. Science (80-.) 305, 994–997. https://doi.org/10.1126/science.1098704.

Mishra, V., Lilhare, R., 2016. Hydrologic sensitivity of Indian sub-continental river basins to climate change. Glob. Planet. Change 139, 78–96. https://doi.org/10.1016/j.gloplacha.2016.01.003.

Mishra, V., Shah, H.L., Kumar, R., Samaniego, L., Eisner, S., Yang, T., 2016. Multimodel assessment of sensitivity and uncertainty of water availability under climate change. Submitt. Clim. Change. https://doi.org/10.1007/s10584-016-1886-8.

Monteith, J.L., 1972. Solar radiation and productivity in tropical ecosystems. J. Appl. Ecol. 9, 747. https://doi.org/10.2307/2401901.

Mu, Q., Zhao, M., Running, S.W., 2013. MODIS Global Terrestrial Evapotranspiration (ET) Product (MOD16A2/A3) – ATBD Collection 5. Missoula.

Mu, Q., Heinsch, F.A., Zhao, M., Running, S.W., 2007. Development of a global evapotranspiration algorithm based on MODIS and global meteorology data. Remote Sens. Environ. 111, 519–536. https://doi.org/10.1016/j.rse.2006.07.007.

Mu, Q., Zhao, M., Running, S.W., 2011. Improvements to a MODIS global terrestrial evapotranspiration algorithm. Remote Sens. Environ. 115, 1781–1800. https://doi.org/10.1016/j.rse.2011.02.019.

Nayak, R.K., Patel, N.R., Dadhwal, V.K., 2013. Inter-annual variability and climate control of terrestrial net primary productivity over India. Int. J. Climatol. 33, 132–142. https://doi.org/10.1002/joc.3414.

Niu, S., Xing, X., Zhang, Z., Xia, J., Zhou, X., Song, B., Li, L., Wan, S., 2011. Water-use efficiency in response to climate change: from leaf to ecosystem in a temperate steppe. Glob. Change Biol. 17, 1073–1082. https://doi.org/10.1111/j.1365-2486.2010.02280.x.

Pai, D.S., Sridhar, L., Rajeevan, M., Sreejith, O.P., Satbhai, N.S., Mukhopadhyay, B., 2014. Development of a new high spatial resolution (0.25° × 0.25°) long period (1901–2010) daily gridded rainfall data set over India and its comparison with existing data sets over the region. Mausam 65, 1–18.

Ponce Campos, G.E., Moran, M.S., Huete, A., Zhang, Y., Bresloff, C., Huxman, T.E., Eamus, D., Bosch, D.D., Buda, A.R., Gunter, S.A., Scalley, T.H., Kitchen, S.G., McClaran, M.P., McNab, W.H., Montoya, D.S., Morgan, J.A., Peters, D.P.C., Sadler, E.J., Seyfried, M.S., Starks, P.J., 2013. Ecosystem resilience despite large-scale altered hydroclimatic conditions. Nature 494, 349–352. https://doi.org/10.1038/nature11836.

Roxburgh, S.H., Berry, S.L., Buckley, T.N., Barnes, B., Roderick, M.L., 2005. What is NPP? Inconsistent accounting of respiratory fluxes in the definition of net primary production. Funct. Ecol. 19, 378–382. https://doi.org/10.1111/j.1365-2435.2005.00983.x.

Roxy, M.K., Ghosh, S., Pathak, A., Athulya, R., Mujumdar, M., Murtugudde, R., Terray, P., Rajeevan, M., 2017. A threefold rise in widespread extreme rain events over central India. Nat. Commun. 8, 1–11. https://doi.org/10.1038/s41467-017-00744-9.

Running, S.W., Nemani, R.R., Heinsch, F.A., Zhao, M., Reeves, M., Hashimoto, H., 2004. A continuous satellite-derived measure of global terrestrial primary production. Bioscience 54, 547–560. https://doi.org/10.1641/0006-3568(2004) 054.

Shah, H.L., Mishra, V., 2016. Hydrologic changes in Indian subcontinental river basins (1901–2012). J. Hydrometeorol. 17, 2667–2687. https://doi.org/10.1175/JHM-D-15-0231.1.

Sharma, A., Goyal, M.K., 2018. Assessment of ecosystem resilience to hydroclimatic disturbances in India. Glob. Change Biol. 24 (2), e432–441. https://doi.org/10.1111/gcb.13874.

Sharma, S., Mujumdar, P., 2017. Increasing frequency and spatial extent of concurrent meteorological droughts and heatwaves in India. Sci. Rep. 7, 15582. https://doi.org/10.1038/s41598-017-15896-3.

Song, Q.-H., Fei, X.-H., Zhang, Y.-P., Sha, L.-Q., Liu, Y.-T., Zhou, W.-J., Wu, C.-S., Lu, Z.-Y., Luo, K., Gao, J.-B., Liu, Y.-H., 2017. Water use efficiency in a primary subtropical evergreen forest in Southwest China. Sci. Rep. 7, 43031. https://doi.org/10.1038/srep43031.

Tang, X., Li, H., Desai, A.R., Nagy, Z., Luo, J., Kolb, T.E., Olioso, A., Xu, X., Yao, L., Kutsch, W., Pilegaard, K., Köstner, B., Ammann, C., 2014. How is water-use efficiency of terrestrial ecosystems distributed and changing on Earth? Sci. Rep. 4, 7483. https://doi.org/10.1038/srep07483.

Thomey, M.L., Collins, S.L., Vargas, R., Johnson, J.E., Brown, R.F., Natvig, D.O., Friggens, M.T., 2011. Effect of precipitation variability on net primary production and soil respiration in a Chihuahuan Desert grassland. Glob. Change Biol. 17, 1505–1515. https://doi.org/10.1111/j.1365-2486.2010.02363.x.

Turner, D.P., Ritts, W.D., Cohen, W.B., Gower, S.T., Running, S.W., Zhao, M., Costa, M.H., Kirschbaum, A.A., Ham, J.M., Saleska, S.R., Ahl, D.E., 2006. Evaluation of MODIS NPP and GPP products across multiple biomes. Remote Sens. Environ. 102, 282–292. https://doi.org/10.1016/j.rse.2006.02.017.

Walker, B., Salt, D., 2006. In: Resilience Thinking: Sustaining Ecosystems and People in a Changing World. Island Press, Washington, DC. https://doi.org/10.2174/1874282300802010217.

Walker, B., Salt, D., 2013. A crash course in the science of resilience. In: Lerch, D. (Ed.), The Community Resilience Reader: Essential Resources for an Era of Upheaval. Island Press, Washington, DC, pp. 163–178. https://doi.org/10.5822/978-1-61091-861-9_10.

Wheeler, T., Braun, J. Von, 2013. Climate change impacts on global food security. Science (80-.) 341, 508–513.

Xu, C., Liu, H., Anenkhonov, O.A., Korolyuk, A.Y., Sandanov, D.V., Balsanova, L.D., Naidanov, B.B., Wu, X., 2017. Long-term forest resilience to climate change indicated by mortality, regeneration, and growth in semiarid southern Siberia. Glob. Change Biol. 23, 2370–2382. https://doi.org/10.1111/gcb.13582.

Xue, B.-L., Guo, Q., Otto, A., Xiao, J., Tao, S., 2015. Global patterns, trends, and drivers of water use efficiency from 2000 to 2013. Ecosphere 6, 1–18. https://doi.org/10.1890/ES14-00416.1.

Yang, Y., Guan, H., Batelaan, O., McVicar, T.R., Long, D., Piao, S., Liang, W., Liu, B., Jin, Z., Simmons, C.T., 2016. Contrasting responses of water use efficiency to drought across global terrestrial ecosystems. Sci. Rep. 6, 23284. https://doi.org/10.1038/srep23284.

Yu, G., Chen, Z., Piao, S., Peng, C., Ciais, P., Wang, Q., Li, X., Zhu, X., 2014. High carbon dioxide uptake by subtropical forest ecosystems in the East Asian monsoon region. Proc. Natl. Acad. Sci. 111, 4910–4915. https://doi.org/10.1073/pnas.1317065111.

Zhang, X., Susan Moran, M., Zhao, X., Liu, S., Zhou, T., Ponce-Campos, G.E., Liu, F., 2014. Impact of prolonged drought on rainfall use efficiency using MODIS data across China in the early 21st century. Remote Sens. Environ. 150, 188–197. https://doi.org/10.1016/j.rse.2014.05.003.

Zhao, M., Heinsch, F.A., Nemani, R.R., Running, S.W., 2005. Improvements of the MODIS terrestrial gross and net primary production global data set. Remote Sens. Environ. 95, 164–176. https://doi.org/10.1016/j.rse.2004.12.011.

Zhao, M., Running, S.W., 2010. Drought-induced reduction in global terrestrial net primary production from 2000 through 2009. Science (80-.) 329, 940–943. https://doi.org/10.1126/science.1192666.

Zhao, M., Running, S.W., Nemani, R.R., 2006. Sensitivity of Moderate Resolution Imaging Spectroradiometer (MODIS) terrestrial primary production to the accuracy of meteorological reanalyses. J. Geophys. Res. Biogeosci. 111, 1–13. https://doi.org/10.1029/2004JG000004.